Supplemental Information

Thermal Conductivity of Suspended Graphene with Defects

Hoda Malekpour[†], Pankaj Ramnani[‡], Srilok Srinivasan[§], Ganesh Balasubramanian[§], Denis L. Nika[†‖], Ashok Mulchandani[‡], Roger Lake[¶] and Alexander A. Balandin[*†]

[†]Phonon Optimized Engineered Materials (POEM) Center and Nano-Device Laboratory (NDL), Department of Electrical and Computer Engineering, University of California – Riverside, Riverside, California 92521 USA

[‡]Department of Chemical and Environmental Engineering, Bourns College of Engineering, University of California – Riverside, Riverside, California 92521 USA

[§]Department of Mechanical Engineering, Iowa State University, Ames, Iowa 50011, USA

[‖]E. Pokatilov Laboratory of Physics and Engineering of Nanomaterials, Department of Physics and Engineering, Moldova State University, Chisinau MD-2009, Republic of Moldova

[¶]Laboratory for Terascale and Terahertz Electronics (LATTE), Department of Electrical and Computer Engineering, University of California – Riverside, Riverside, California 92521 USA

In this paper we report on the investigation of thermal conductivity of suspended CVD-grown graphene with e-beam induced defects. For this study, defects where induced controllably through low energy electron beam irradiation at different steps, and the optothermal Raman technique was used to measure the thermal conductivity after each step of irradiation. In this Supplementary Information document, we present additional data on crystallinity of CVD grown graphene as well as details of thermal conductivity measurement performed on suspended single layer graphene at different steps of irradiation. We also explain how the nature of e-beam induced defects was investigated using Raman spectroscopy.

Assessment of Quality of Graphene Grown by Chemical Vapor Deposition

We have verified that CVD graphene was either single crystal or with large crystalline grains that preserved global crystallographic orientation. The defects confirmed by Raman studies

mostly resulted from the transfer process. The single layer graphene samples were synthesized using ambient pressure chemical vapor deposition (AP-CVD). The ultralow concentration of methane (90 ppm) decreases the nucleation density of the growth seeds of graphene. This low nucleation density, in turn, allows for growth of large-sized single crystalline grains of graphene and minimizes grain boundaries by preventing overlapping of graphene grains. The typical SEM micrographs of graphene grown on Cu foil at UC Riverside are shown in Fig. S1 (a, b). The crystalline nature of the graphene was further confirmed using selected area electron diffraction (SAED) pattern (Fig. S1 (c)) and high resolution-transmission electron microscopy (HR-TEM) (Fig. S1 (d)). The clear diffraction spots and the absence of any diffused rings are indicative of single crystallinity or large-grain size of graphene.

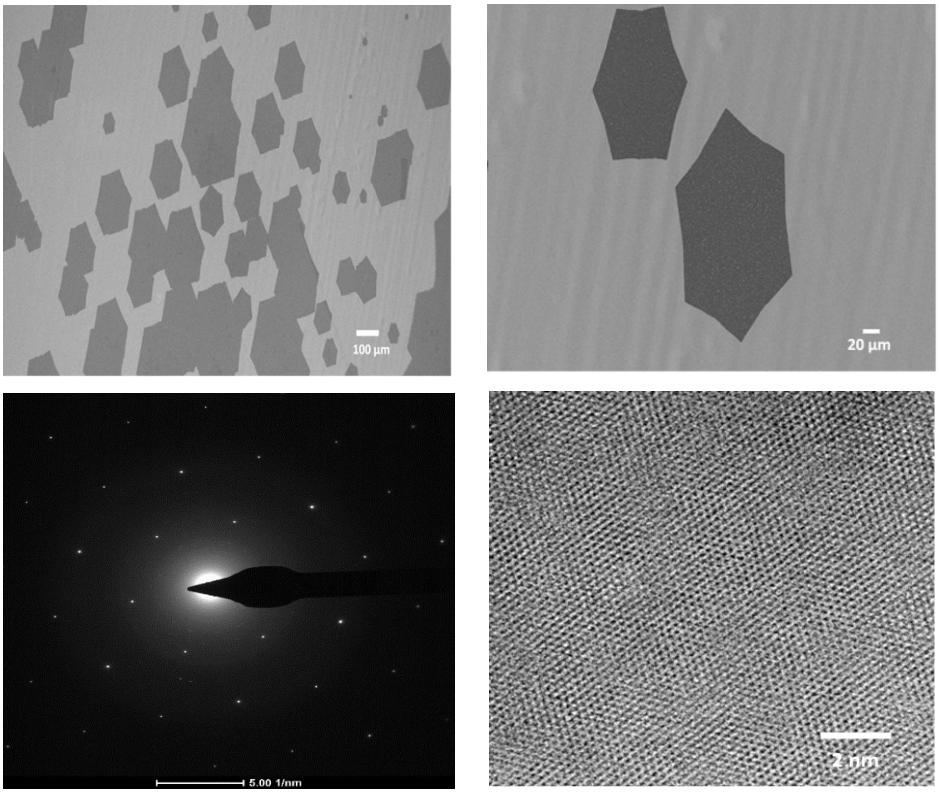

Figure S1 (a, b) SEM image of high-quality graphene grown on Cu foil, (c) Selected area electron diffraction (SAED) pattern using FEI Titan Themis 300, (d) Bright-field high resolution- transmission electron micrograph (HR-TEM) of the single crystalline graphene

Optothermal Raman Measurements

In this technique, the Raman spectrometer performs first as a heater, causing local heating at the laser spot, and second as a thermometer, measuring the temperature rise from the Raman G-peak shift, caused by the laser heating [S2]. The graphene possesses clear G and 2D Raman bands, therefore the temperature could be accurately read. The dependence of the G-peak shift on the temperature and total power is presented in Figs. S2 and S3, respectively. For power levels below 2 mW, the D-to-G peak ratio was almost independent of the power. The slope factor of the G-peak shift was extracted in this power range. Figure S4 shows the dependence of Raman D to G peak intensity ratio for highly irradiated graphene sample for powers ranging up to 3 mW. When the laser power exceeds 2 mW local annealing of induced defects can occur leading to Raman D to G peak intensity ratio decrease.

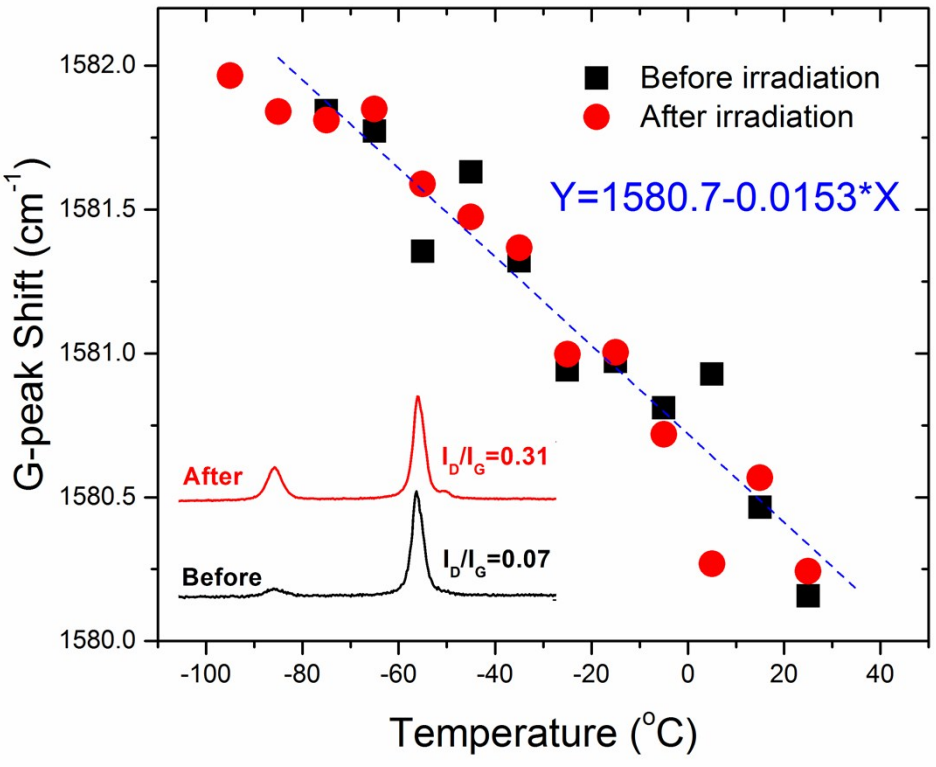

Figure S2 Calibration measurement done on SLG#2 before and after the irradiation procedure. The temperature coefficient of the Raman G-peak are not affected by irradiation and can be assumed constant.

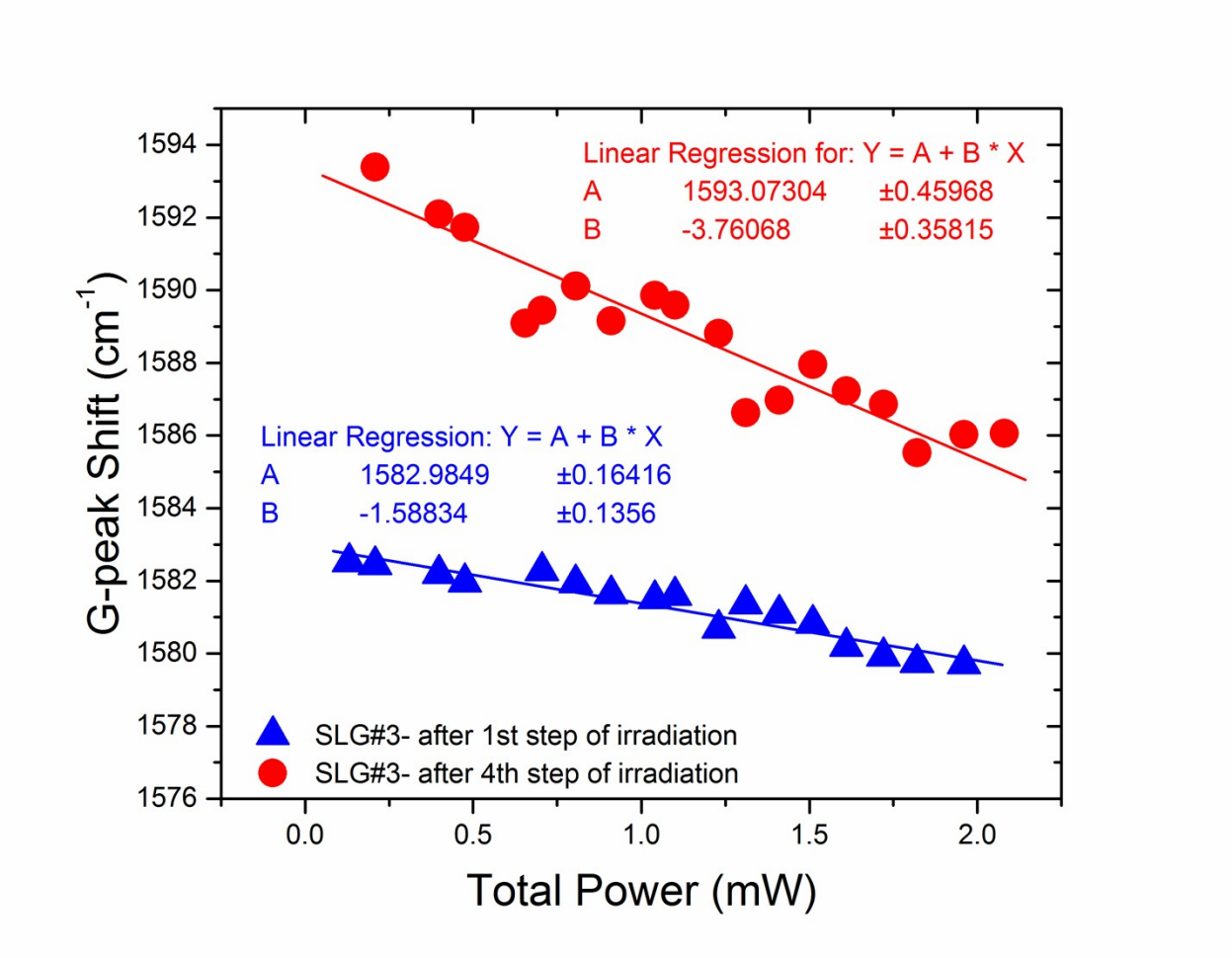

Figure S3 Power dependent Raman measurement results shown for SLG #3 after the 1st and 4th steps of irradiation were applied. One should notice the increase of the slope factor, which is directly related to the suppression of thermal conductivity. The power range has been kept below 2 mW to avoid local healing of induced defects.

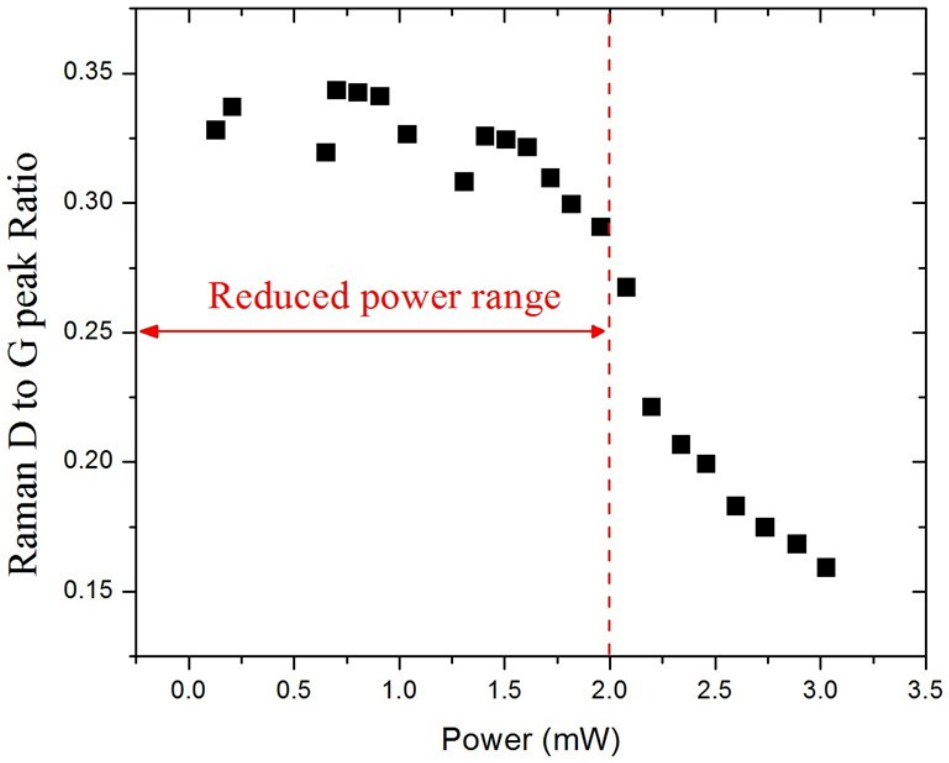

Figure S4 Raman D to G peak intensity ratio as a function of the excitation power.

Thermal Conductivity Extraction Procedure

Fourier's equation was solved in a two-dimensional structure for our specific sample geometry in order to extract thermal conductivity. COMSOL Multiphysics software package was used to numerically solve the heat diffusion equation under corresponding boundary conditions. We have assumed a Gaussian heat distribution of power for our laser spot heat source. The power distribution function, $P(x,y)$, through the sample is given as:

$$P(x,y) = \frac{P_{abs}}{2\pi\sigma} exp(-\frac{x^2+y^2}{2\sigma^2}) \quad \text{(S1)}$$

Here P_{abs} is the absorbed power by the sample, which itself is equal to $\alpha\% \times P_{tot}$ (α and P_{tot} denote the absorption coefficient and total laser power on the sample, respectively). σ is the

standard deviation of our Gaussian heat distribution function which is defined based on our laser spot size. Knowing excitation wavelength (λ) and the objective numerical aperture (NA), one can directly calculate the laser spot size: $2\lambda/\pi \times NA$. For our case, using 488 nm laser excitation under 100X objective with the numerical aperture of 0.85 the laser spot size would be 0.36 μm. The full width at half maximum of the Gaussian function is then set to the laser spot size, giving σ the value of 0.15 μm. The suspended graphene flake over a 7.5 μm square hole meets the gold heat sink at all four boundaries. The heat sink was assumed to be ideal and the thermal resistance between graphene and gold substrate was neglected; therefore the heat sink was modeled by defining a constant room temperature (300K) for the square sample's four boundaries. The iteration procedure was then used to solve heat diffusion equation by giving the total power and thermal conductivity as inputs to our model and getting the samples temperature distribution as the output. The output was then corrected based on the measured temperature in laser spot by adjusting thermal conductivity to lower or higher values. This adjustment was simplified by introducing the slope parameter:

$$\theta = \frac{\partial \omega}{\partial P} = \chi \frac{\partial T}{\partial P} \quad \text{(S2)}$$

By plotting K versus θ, thermal conductivity can be easily extracted having the slope parameter from experiment. A sample of this plot is shown in Fig. S5.

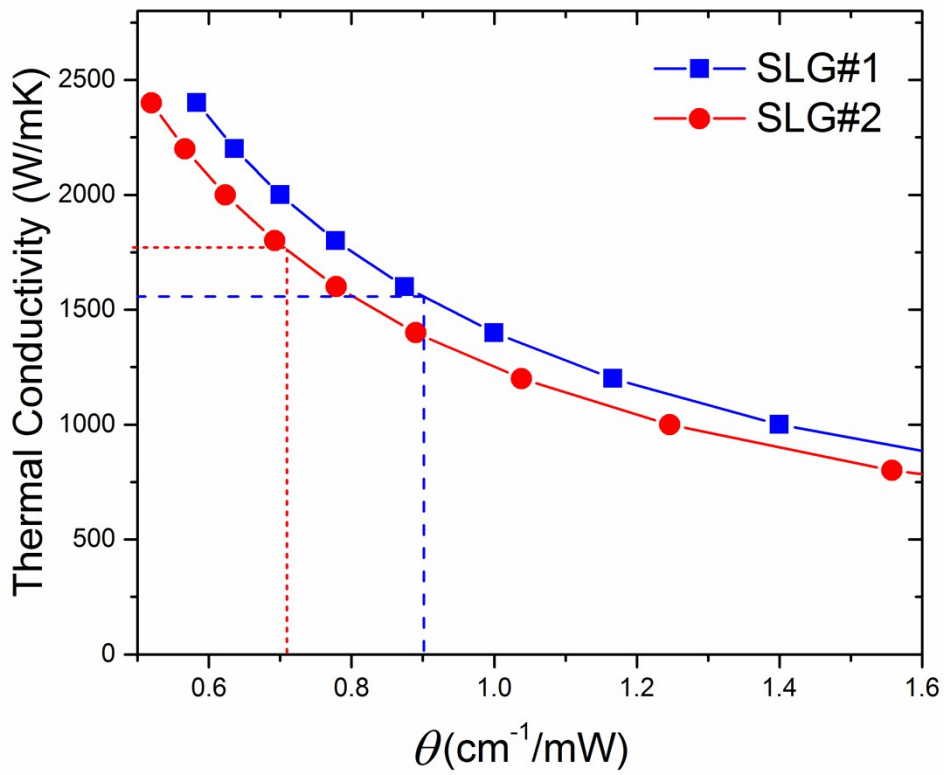

Figure S5 Typical simulation results obtained from our COMSOL modeling showing the θ factor. Thermal conductivity can be directly extracted by just having power dependent Raman measurement slope.

Analysis of Defects in Graphene Using Raman Spectroscopy

Based on the resonant Raman theory, it is known that at low defect concentration, the intensity ratio of the Raman D to D' peak is independent of the defect concentration and is related to the nature of the defects [S2]. Following this fact, Eckmann et al. experimentally investigated the correspondence of Raman D to D' band intensity ratio for different types of defects in graphene [S3]. In order to perform the analysis, a Lorentzian function was fitted to Raman D and G bands and a Fano line shape to Raman D' band. Using their methodology, we found out that our irradiated graphene sample showed I(D)/I(D') ~7 corresponding to the vacancy type defects (see Fig. S6).

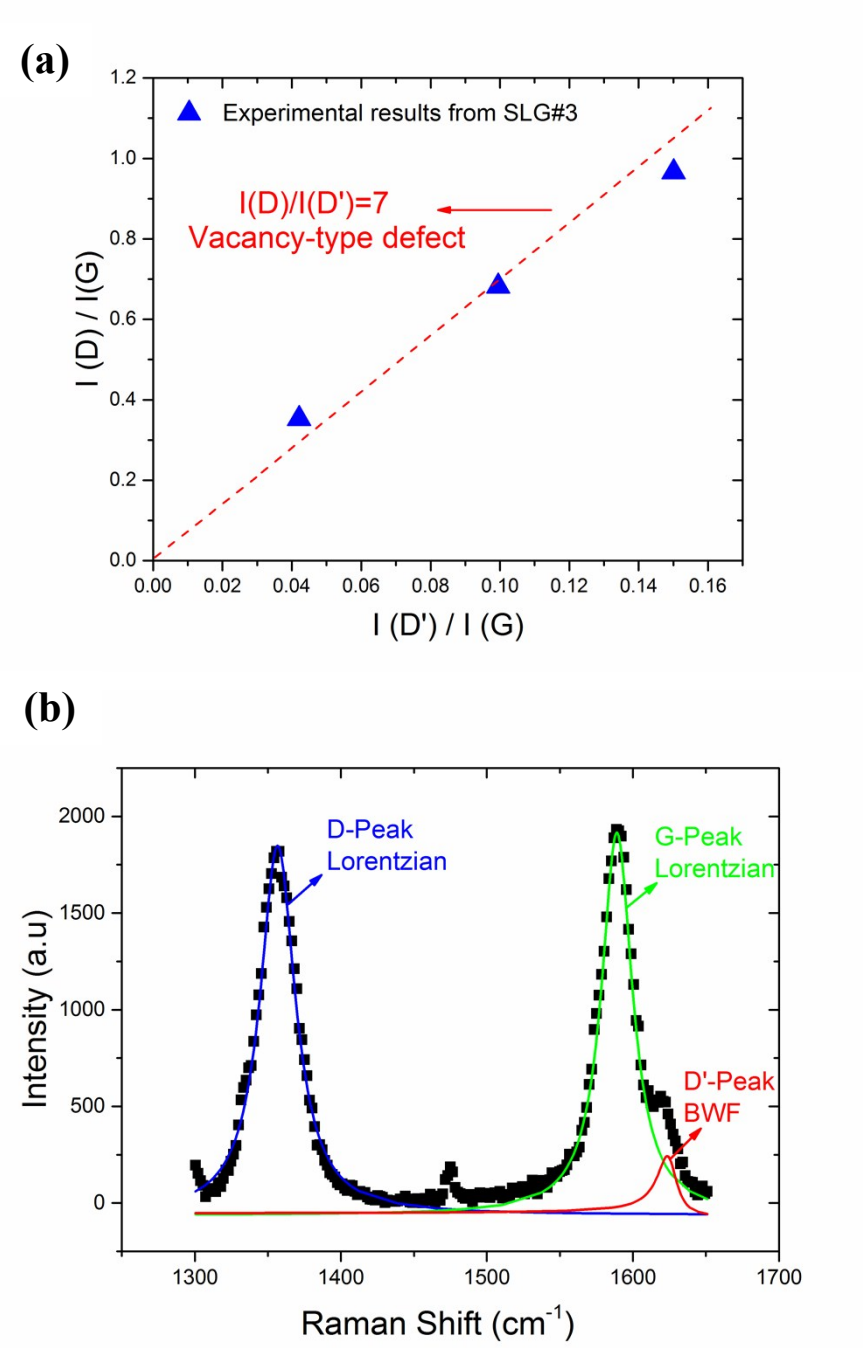

Figure S6: (a) Nature of defects has been found to be mostly vacancies based their Raman spectrum analysis. The Raman D to D' peak intensity ratio of ~7 has been achieved, for SLG #3 at different steps of irradiations, which has been attributed to vacancy type defect [H13]. (b) The details of Raman peak analysis for extracting nature of defects: Raman D and G peak was fitted with Lorentzian function while D' peak was fitted using Fano line shape.

References

[S1] Balandin, A. A. *Nature Materils* **2011**, *10*, 569 - 581.

[S2] Venezuela, P.; Lazzeri, M.; Mauri, F. *Phys. Rev. B* **2011**, *84* (3), 035433.

[S3] Eckmann, A.; Felten, A.; Mishchenko, A.; Britnell, L.; Krupke, R.; Novoselov, K. S.; Casiraghi, C. *Nano Lett.* **2012**, *12* (8), 3925-3930.